Proceedings of ASME Turbo Expo 2011
GT2011
June 6-10, 2011, Vancouver, British Columbia, Canada

GT2011-45059

THE COST OF FLOW CONTROL IN A COMPRESSOR

Simon W. Evans
Worcester Polytechnic Institute
Worcester, MA, 01609, USA

Howard P. Hodson
Whittle Laboratory,
University of Cambridge, UK

ABSTRACT

This paper documents an analysis performed to estimate the cycle cost of flow control in a compressor. The analysis is based on a series of experiments conducted in a low-speed compressor cascade at high incidence. In these experiments, flow control was applied to delay a turbulent separation on the suction surfaces of the blades in the cascade. The flow control methods studied include boundary layer suction and both steady and pulsed vortex generator jets. Endwall control was also applied to remove corner separations. Tip gaps and endwall suction were both studied for this purpose. The flow control methods studied were able to successfully delay a separation occurring on the suction surface of the blades, reducing the loss coefficient. The mass flow rates and jet supply pressures required to achieve control in each case were used to model a single flow-controlled blade row in a typical turbofan cycle using cycle analysis software. The cost of control to the cycle was calculated as the polytropic compressor efficiency increase required to maintain thrust relative to a conventional cycle with no flow control. The results of the analysis show that the benefits of flow control significantly out-weigh the cost. They also show that boundary layer suction coupled with endwall suction yields the lowest cycle cost. This is because of the small pressure difference required to drive suction, which allows reinjection of the aspirated air a short distance upstream of the flow controlled blade row.

NOMENCLATURE

A_j	=	Total jet area on one blade [m^2],
AVR	=	Axial velocity ratio,
b	=	Blade span [m],
C_μ	=	Injected momentum coefficient,
f	=	Unsteady actuation frequency [Hz],
F^+	=	Reduced actuation frequency,
GSP	=	Gas Turbine Simulation Program,
l	=	Distance along the suction surface [m]
L	=	Length of the separation region [m],
$\dot{m}$	=	Mass flow rate [kg/s],
MR	=	Mass flow ratio,
NLR	=	Nationaal Lucht- en Ruimtevaartlaboratorium,
p_0	=	Stagnation pressure [Pa],
s	=	Blade pitch [m],
v	=	Local velocity [m/s],
V	=	Velocity [m/s],
VGJ	=	Vortex generator jet,
VR	=	Jet velocity ratio,
Y	=	Loss coefficient,
α	=	Flow angle [°],
ρ	=	Density [kg/m^3].
y	=	pitchwise coordinate
z	=	spanwise coordinate

Subscripts

1	=	Upstream,
2	=	Downstream,
a	=	Averaged over full span,
end	=	Endwall,
j	=	Jet,
$meas$	=	Measured,
p	=	Profile,
s	=	Suction,
te	=	Trailing edge,
∞	=	Freestream.

INTRODUCTION

Flow control has been investigated for application in compressors by a number of researchers [1],[2],[3],[4]. In this application, flow control is applied to delay boundary layer separations occurring on the suction surfaces of highly loaded blades, allowing higher stage loading to be achieved.

Culley *et al* [1] and Kirtley *et al* [2] both applied control using direct streamwise injection to delay separations occurring on the suction surface of highly loaded blades within rotating compressor rigs. In the work of Culley *et al* [1], flow control was used to delay a laminar boundary layer separation on the suction surface of re-staggered vanes in a low-speed compressor facility. Flow control was shown to reduce the area-averaged stagnation pressure loss through the blade row by 25%, relative to the uncontrolled, re-staggered case. In the work of Kirtley *et al* [2], the solidity of the stator blade row was reduced by 30% relative to its baseline, yielding a 25% increase in diffusion factor and causing a turbulent boundary layer separation on the blade suction surfaces. The application of flow control delayed this separation, yielding a loss reduction relative to the baseline case. Both experiments showed a loss reduction with a fraction of inlet mass flow rate injected into the flow of 1%. In the work of Culley *et al*, the quoted level of control authority was achieved with a pulsed jet, while in the work of Kirtley *et al*, a steady jet was used.

These experiments prove that flow control can be used to reduce the loss coefficient and increase the loading of a highly loaded blade row. In order to evaluate the viability of flow control within a compressor, however, the cost to the cycle must be identified in addition to the possible benefits. This cost has many components, including the cost of manufacturing a hollow, flow-controlled blade and the need for the hollow blades to be made from stronger, more expensive materials. The main cost component, however, is the impact of flow control on operating costs. This is associated with the cost of control on the engine cycle and it is this cost that is the topic of this paper.

In the case of control by blowing, the cost to the cycle can be reduced by reducing the injected mass flow rate, as this mass flow must be bled from the aft part of the compressor where the pressure is sufficient to drive the control jets at their required velocity. Pulsing the jet is one way to achieve such a mass flow reduction, while maintaining the same level of control authority. Vortex generator jets (VGJs) are another. Vortex generator jets create streamwise vortices that mix the freestream with the inner boundary layer, re-energizing regions of separated flow if placed appropriately relative to the separation. Since the inner boundary layer is re-energized with freestream momentum rather than jet momentum, a reduction in jet momentum is possible over the direct streamwise injection method of flow-control. Furthermore, vortex generator jets may also be pulsed.

In previous work, the authors and co-workers [4] have explored both steady and pulsed vortex generator jets on a flat plate with the pressure distribution of a separating compressor blade suction surface imposed upon it. Using trailing edge boundary layer measurements, an equivalent loss coefficient representing a cascade at high incidence was calculated with and without the application of flow control. With steady vortex generator jets, a loss reduction of 36% was calculated for a jet mass flow rate of 0.13% of the inlet mass flow rate. By pulsing the jets, this mass flow rate was reduced to 0.08%, but a higher peak jet velocity was required than the steady blowing case. This is important when considering the cost of flow control, as a higher peak jet velocity means that the air supplying the jet must be bled from a higher source pressure supplied from further aft in the compressor, which is more costly to the cycle.

Another flow control approach that has been explored in the application of compressors is boundary layer suction [5],[6]. By removing low momentum fluid from the near wall region, a fuller boundary layer velocity profile is promoted and the onset of separation delayed. Although this technique does not require air to be bled from downstream in the compressor, the aspirated air must be dumped somewhere, and does therefore affect the cycle.

In addition to the cost associated with flow control applied to the suction surface, an increase in loading increases the extent of hub-corner separations in rotors and shrouded stators. Similar behavior has been widely observed on the endwalls of linear compressor cascades. Gbadebo *et al* [7] showed that the thickness of the separated flow region increases as the incidence of the blade is increased. Blockage and loss increase accordingly. A number of approaches for the control of corner separations are documented in the literature including tip gaps [8],[9],[10], passive vortex generators [11], pulsed jets [12], synthetic jets [13] and endwall suction [10],[14]. Tip gaps and endwall suction have been more effective to date than the other techniques, both completely removing the corner separations when implemented correctly [3],[10].

In this paper three forms of suction surface boundary layer control are investigated together with two forms of endwall control. On the blade suction surfaces, these include steady and pulsed blowing through vortex generator jets, and boundary layer suction. In the suction surface/endwall corners, tip gaps and endwall suction are investigated.

EXPERIMENTAL FACILITY

The experiments were conducted in a linear cascade of 7 blades located on the exit of a low-speed, continuous, blower-type wind tunnel at the Whittle Laboratory, University of Cambridge. The blade profile was designed by MTU Aero Engines to have the same pressure coefficient distribution at low speed as a conventional compressor blade at high speed. Since the blade is not a highly loaded blade, separation was achieved on the suction surface by increasing the incidence. For the experiments discussed here, the incidence was fixed at 12.5°, corresponding to an inlet flow angle was 49°. Details of the cascade are included in Table 1. The experiments were conducted at a Mach Number of 0.07 and a chord based Reynolds Number of 0.5×10^6. The blade chord of 325 mm was chosen to yield this Reynolds Number given the maximum velocity of the wind tunnel. With the geometry of the tunnel, this resulted in an aspect ratio of 1.9. Measurements were taken one chord downstream of the cascade, as indicated in a schematic of the cascade shown in Figure 1. Loss measurements were taken over one blade pitch downstream of the center blade – blade 4 in Figure 1. This blade was also instrumented with static pressure tappings. More details of the facility can be found in Evans [15].

Each blade contains one row of jet holes located at 54% chord (61% suction surface length, l_{te}) on the suction surface. The jet holes are 4 mm in diameter, pitched at 30º to the surface and skewed at 60º to the freestream direction as shown schematically in Figure 2. This skew angle has been shown to yield a greater loss reduction over a wide range of jet blowing velocities than jets skewed at either 45º or 90º [4]. Skewed jets have been shown to produce a row of co-rotating streamwise vortices [16]. Selby *et al* [17] have shown that these yield a better pressure recovery downstream of a separation than the counter-rotating vortex pairs produced by normal jets or jets with alternating skew direction. For boundary layer suction, the same holes were used as for blowing.

Table 1. Description of the cascade

Chord	325 mm
Solidity	1.53
Aspect ratio	1.9
Inlet flow angle	49º
Incidence	12.5º
Inlet Mach Number	0.07
Reynolds' number	0.5×10^6

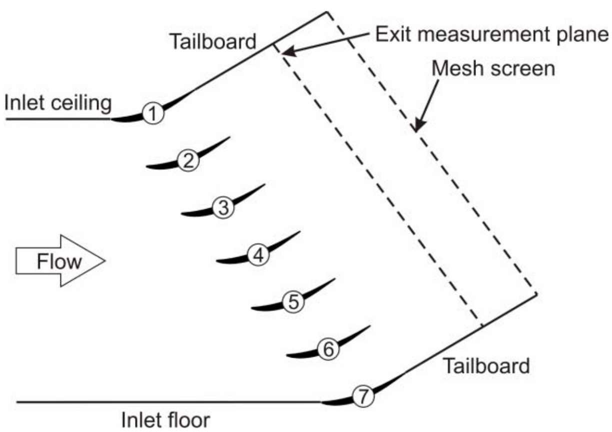

Figure 1. Schematic of linear compressor cascade.

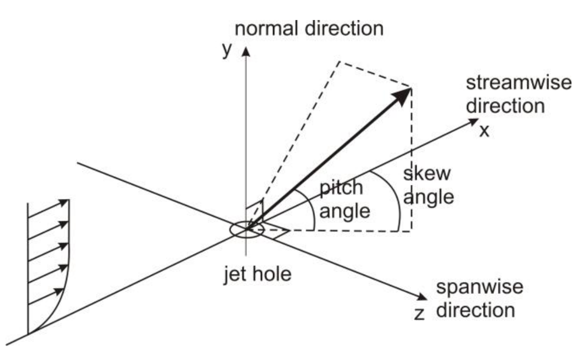

Figure 2. Vortex generator jet orientation.

The jets were supplied with air from the laboratory air system via external pipes and channels within the blades. Jet mass flow rates were measured using a flow meter located in the air supply line to each blade. The flow meter had a resolution of 2 lpm, giving a measurement uncertainty of 0.7% in flow rate measurements. The internal geometry of the blade was designed so that all jets were in phase when pulsed. A rotating siren valve was used to produce the pulsed jets. The pulsed jet velocity variation was measured using a hotwire anemometer located in one jet hole. This anemometer was calibrated *in situ* using the mass flow rate measured with the flow meter.

Downstream measurements were taken with a Neptune probe, combining a static pressure probe and a three-hole probe, similar to the design of Sieverding *et al* [18]. Pressures were measured using a Pressure Systems International (PSI) *Netscanner 9160*.

DATA ANALYSIS AND REDUCTION

The metric used to evaluate the performance of flow control is the mixed-out stagnation-to-stagnation pressure loss coefficient. Two loss coefficients were calculated – the mixed-out midspan profile loss coefficient and the mixed-out loss coefficient averaged over the full blade span. The latter is important as it includes the impact of suction surface flow control on the corner separations and also accounts for endwall control. The profile loss coefficient, Y_p, is defined in equation (1) in terms of a measured loss coefficient $Y_{meas,p}$, a jet loss coefficient, Y_j, and a suction loss coefficient, Y_s. The measured loss coefficient is defined in equation (2) in terms of the mixed-out stagnation pressure measured over one blade pitch at midspan, p_{02}. The jet loss coefficient is defined in equation (3) and accounts for the mixing of the vortex generator jets with the free-stream. The suction loss coefficient, defined in equation (4), accounts for the losses associated with air removed from the blade surface in those cases in which boundary layer suction was applied. The jet and suction loss coefficients are defined in terms of the ratios of injected or aspirated mass flow rates, $\dot{m}_j$ and $\dot{m}_s$ respectively, to the mass flow rate downstream of the cascade, $\dot{m}_2$.

$$Y_p = Y_{meas,p} + Y_j + Y_s \tag{1}$$

$$Y_{meas,p} = \frac{p_{01} - p_{02}}{\frac{1}{2}\rho V_1^{\,2}} \tag{2}$$

$$Y_j = \left(\frac{\dot{m}_j}{\dot{m}_2}\right)\left(\frac{p_{0j} - p_{02}}{\frac{1}{2}\rho V_1^{\,2}}\right) \tag{3}$$

$$Y_s = -\left(\frac{\dot{m}_s}{\dot{m}_2}\right)\left(\frac{p_{0s} - p_{02}}{\frac{1}{2}\rho V_1^{\,2}}\right) \tag{4}$$

The area loss coefficient, Y_a, is defined in equation (5) in terms of a measured loss coefficient, $Y_{meas,a}$, a jet loss coefficient, Y_j, a suction loss coefficient, Y_s, and an endwall suction loss coefficient, $Y_{s,end}$. The measured loss coefficient is defined in equation (6) in terms of the mixed-out stagnation pressure mass averaged over the full blade span, p_{02a}. The jet and suction loss coefficients are defined in equations (7) and (8) respectively, while the endwall suction loss coefficient is defined in equation (9) in terms of the endwall suction mass flow rate, $\dot{m}_{s,end}$, and the suction pressure, $p_{0s,end}$.

$$Y_a = Y_{meas,a} + Y_j + Y_s + Y_{s,end} \tag{5}$$

$$Y_{meas,a} = \frac{p_{01} - p_{02a}}{\frac{1}{2}\rho V_1^2} \tag{6}$$

$$Y_j = \left(\frac{\dot{m}_j}{\dot{m}_2}\right)\left(\frac{p_{0j} - p_{02a}}{\frac{1}{2}\rho V_1^2}\right) \tag{7}$$

$$Y_s = -\left(\frac{\dot{m}_s}{\dot{m}_2}\right)\left(\frac{p_{0s} - p_{02a}}{\frac{1}{2}\rho V_1^2}\right) \tag{8}$$

$$Y_{s,end} = -\left(\frac{\dot{m}_{s,end}}{\dot{m}_2}\right)\left(\frac{p_{0s,end} - p_{02a}}{\frac{1}{2}\rho V_1^2}\right) \tag{9}$$

Since the aim of flow control in this application is the removal of flow separations, the blockage is also affected by flow control. Blockage, B, is defined for the full flow passage in equation (10).

$$B = \iint \left(1 - \frac{v}{V_\infty}\right) dz dy \tag{10}$$

where, z and y are the coordinates in the spanwise and pitchwise directions respectively, v is the local velocity, and V_∞ is the freestream velocity through the passage. The resolution of this integral was 10 mm in the y direction and between 5 mm and 20 mm in the z direction.

When using blowing, the cost of flow control to the cycle is a function of the mass flow rates of air required to be bled from downstream stages. The jet mass flow rate is therefore another parameter that is important for the evaluation of flow control, quoted in equation (11) as a mass flow ratio, MR, in which the jet mass flow rate is normalized by the passage inlet mass flow rate. This definition assumes constant density and rectangular velocity profiles. Also important is the jet velocity itself, which establishes the required supply pressure. Jet velocity is quoted in equation (12) as a velocity ratio, VR, in which the jet velocity is normalized by the cascade inlet velocity. The effectiveness of flow control by blowing is more closely related to jet momentum than jet mass flow or velocity, however. An injected momentum coefficient, C_μ, is defined in equation (13). This definition is also based on assumptions of constant density and rectangular velocity profiles.

$$MR = \frac{A_j}{bs\cos(\alpha_1)}\left(\frac{V_j}{V_1}\right) \tag{11}$$

$$VR = \frac{V_j}{V_1} \tag{12}$$

$$C_\mu = \frac{2A_j}{bs\cos(\alpha_1)}\left(\frac{V_j}{V_1}\right)^2 \tag{13}$$

EXPERIMENTAL RESULTS

The baseline cascade, with no control on the blade suction surfaces or endwalls did not experience midspan boundary layer separation. This was due to the presence of corner separations that created large loss cores downstream of the suction surface/endwall corners. These are evident in Figure 3, which plots the measured loss coefficient defined in terms of the local stagnation pressure, p_{02}, over an area defined by the blade span and one blade pitch. Measurement locations are shown as '+' symbols. The corner separations created blockage at the ends of the blades causing the streamtube to contract in the spanwise direction as it passed from the leading edge to the trailing edge of the blade. Evidence of this contraction is an axial velocity ratio (AVR) measured at midspan of 1.07. This contraction caused an acceleration that off-loaded the midspan, preventing the separation expected from 2-D CFD analysis. The midspan profile loss coefficient, Y_p, measured in this case is 0.034, while the area loss coefficient, Y_a, is 0.132.

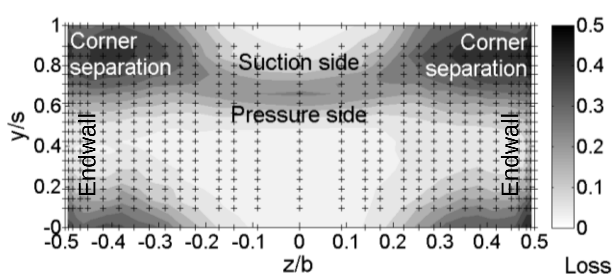

Figure 3. Measured loss contours one chord downstream of cascade for case with no suction surface or endwall control. Measurement locations shown as '+' symbols.

Endwall Control

In order to eliminate the corner separations causing the loss cores shown in Figure 3, endwall control was applied to the cascade. Two forms of endwall control were studied – tip gaps and endwall suction. Both yielded effective control of the endwalls, eliminating the corner separation and causing the midspan suction surface boundary layer to separate at 54% chord. The separation location was identified from static pressure measurements taken at the midspan of the middle blade in the cascade.

Contours of loss coefficient measured downstream of the cascade are shown in Figure 4 for the two cases with endwall control. Measurement locations are the same as shown in Figure 3 and so are not repeated. Figure 4(a) shows the effect of tip gaps in which the clearance on the end of each blade is 1% of chord, and extends from the leading edge to the trailing edge, as recommended by Gbadebo [10]. The tip gap is only interrupted by locating pins that hold the blades in place and the air supply lines supplying the jet holes. Although loss cores still exist in the endwall regions, downstream of the trailing edge, they are substantially reduced in size relative to the uncontrolled case shown in Figure 3. The thickened midspan boundary layer shown in Figure 4(a) is due to a boundary layer separation identified by static pressure measurements taken on the suction surface. The AVR measured in this case was 1.0, indicating a two-dimensional flow at midspan. The profile loss coefficient, Y_p, has increased to 0.099 due to the midspan separation, while the area loss coefficient, Y_a, has dropped to 0.115.

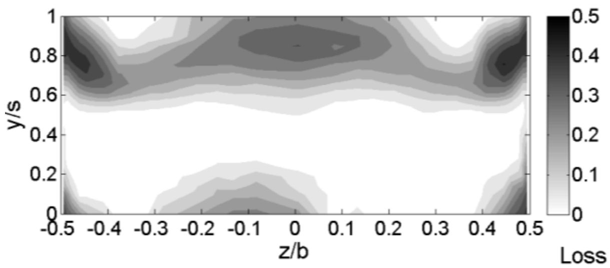

(a)

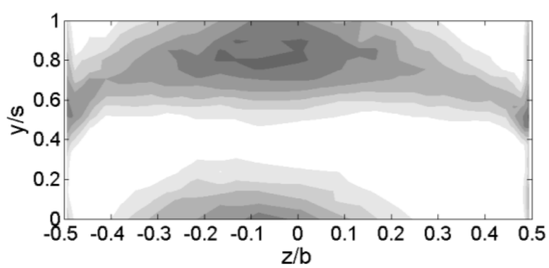

(b)

Figure 4. Measured loss contours one chord downstream of cascade for endwall control by (a) tip gaps, and (b) endwall suction, $\dot{m}_{s,end} / \dot{m}_1$ = 0.7%.

The aspect ratio of the cascade is 1.9. This is low compared with a typical early stage high pressure compressor stator blade, for which 3.5 is more typical. This means that the endwall separations contribute more to the area loss in the cascade than they would in a compressor with a representative aspect ratio. For this reason, the area loss coefficient, Y_a, was corrected for aspect ratio. This correction was performed using equation (14). In this equation, the loss associated with the endwall regions is corrected by multiplying the difference between $Y_{meas,a}$ and $Y_{meas,p}$ by the ratio of the cascade aspect ratio to 3.5. This corrected endwall region loss is then added to the profile loss, which is unchanged by aspect ratio. The loss associated with endwall suction is also corrected, but the jet and boundary layer suction terms are not. This is because these terms are defined in terms of the ratio of total jet area on one blade to the inlet area of the passage. An increase in the aspect ratio will not change this ratio, as more jet holes would be added on the longer blade. The corrected area loss coefficient, $Y_{a,3.5}$, for the case with tip gaps for endwall control is 0.098.

$$Y_{a,3.5} = Y_{meas,p} + Y_j + Y_s + \frac{1.9}{3.5}\left(Y_{meas,a} - Y_{meas,p} + Y_{s,end}\right) \qquad (14)$$

The effect of endwall suction for endwall control is shown in Figure 4(b). The loss cores have been completely removed in this case, again causing a thickening of the midspan wake associated with a suction surface boundary layer separation. Endwall suction was applied through slots located on the endwalls, along the blade suction surface from 45% suction surface length to the trailing edge. The mass flow rate required to eliminate the loss cores was 0.7% of the passage inlet mass flow rate. The profile loss coefficient, Y_p, is 0.069 in this case, lower than measured in the case with tip gaps. The area loss coefficient, Y_a, is 0.087, also lower than measured in the case with tip gaps. Correcting for aspect ratio, $Y_{a,3.5}$ is 0.079.

A summary of the loss coefficients measured in the baseline and endwall control cases is included in Table 2 for ease of reference.

Table 2. Summary of loss coefficients calculated for in baseline and endwall control cases.

Endwall Control	None (Baseline)	Tip Gaps	Endwall Suction
Y_p	0.034	0.099	0.069
$Y_{a,3.5}$	0.087	0.098	0.079

Steady Blowing

By causing the midspan suction surface boundary layer to separate, the application of endwall control creates the opportunity to use flow control on the suction surface to reduce the midspan profile loss coefficient, and accordingly, the area loss coefficient. The first flow control approach studied to achieve this was that of steady blowing with vortex generator jets. These jets were applied to both the cascade with tip gaps and the cascade with endwall suction. The results are summarized in Table 3 along with other cases that will be discussed below. The case with tip gaps for endwall control and vortex generator jets on the suction surface is described as case

1, while two cases with endwall suction and vortex generator jets on the suction surface are described as cases 2 and 3.

Table 3. Summary of cases studied (estimated parameters in italics).

Case #	1	2	3	4	5
Endwall control	Tip Gaps	Fixed endwall suction	Tuned endwall suction	Tip Gaps	Fixed endwall suction
Suction surface control	Steady VGJs	Steady VGJs	Steady VGJs	Pulsed VGJs	Suction
Y_p	0.039	0.026	0.033	0.042	0.037
% Y_p reduction	61.2%	61.8%	51.9%	57.3%	46.2%
$Y_{a,3.5}$	*0.056*	0.064	0.070	-	0.058
% $Y_{a,3.5}$ reduction	*35.9%*	26.5%	20.3%	-	33.9%
$Y_{meas,a}$	*0.070*	0.079	0.053	-	0.057
B	*0.079*	0.053	0.036	-	0.053
V_j/V_1	0.70	0.86	0.89	0.71	-
$\dot{m}_j/\dot{m}_1$	0.18%	0.22%	0.23%	0.12%	-
C_μ	0.28%	0.42%	0.45%	0.18%	-
V_s/V_1	-	-	-	-	0.61
$\dot{m}_s/\dot{m}_1$	-	-	-	-	0.17%
$\dot{m}_{s,end}/\dot{m}_1$	-	0.76%	1.41%	-	0.71%

Tip gaps for endwall control

Static pressure measurements taken at midspan for the case with steady blowing on the suction surface and tip gaps for endwall control showed that the separation was removed from the surface for jet velocity ratios greater than and equal to 0.7. A velocity ratio of 0.7 corresponds to a jet mass flow ratio of 0.18% and an injected momentum coefficient of 0.28%. Figure 5 shows the isentropic surface velocity distribution for this case, as well as the case with tip gaps only. Separation in the case with tip gaps only was identified at 61% suction surface length (54% chord). Figure 5 shows that this separation has been removed from the surface with the velocity ratio of 0.7. The minimum midspan profile loss coefficient, Y_p, achieved with vortex generator jets and tip gaps was 0.039 and corresponded to the jet velocity ratio of 0.7 – the minimum for which no separation was evident in the static pressure measurements. Higher jet velocities did not yield a further loss reduction. This loss coefficient represents a reduction of 61% relative to the case with tip gaps only, described above.

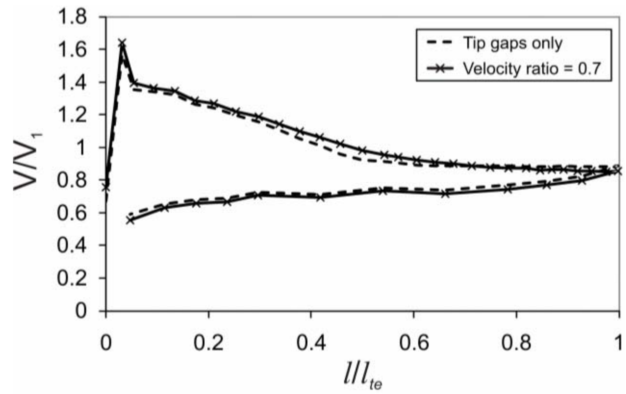

Figure 5. Isentropic surface velocity distributions for case with tip gaps only, and for case with tip gaps for endwall control and vortex generator jets on the suction surface. C_μ = 0.28%, V_j/V_1 = 0.7.

Loss contours downstream of the cascade are shown in Figure 6 for the case with tip gaps for endwall control and vortex generator jets on the suction surface with a jet velocity ratio of 0.9. The thin wake at midspan is consistent with the absence of separation indicated by the static pressure measurements. A large loss core, however, exists on the left-hand endwall. This was found to be the result of a spanwise flow induced by the jets all skewed in the same direction, which aggravated the corner separation on the side of the cascade to which the jets were skewed. The area loss coefficient, Y_a, in this case is 0.075. No area traverse was performed at the jet velocity ratio of 0.7 corresponding to the minimum loss coefficient. The profile loss coefficients in the two cases are similar – 0.039 for a velocity ratio of 0.7 and 0.041 for a velocity ratio of 0.9. This is because the separation has been removed from the suction surface with a velocity ratio of 0.7 and so in increase to 0.9 does not change the boundary layer flow. In light of this result, it is assumed that the full wake is similar in the two cases. The measured loss coefficient, $Y_{meas,a}$, for the velocity ratio of 0.7 is therefore assumed to equal that in the case with a velocity ratio of 0.9. This $Y_{meas,a}$ is 0.070, as quoted in Table 3. It is quoted in italics to indicate that this is an estimated parameter. This results in an area loss coefficient, Y_a, of 0.071. When corrected for aspect ratio, $Y_{a,3.5}$ is 0.056, as quoted in Table 3 (also in italics). This is a 35.9% reduction relative to the baseline case with no endwall or boundary layer control. This number is also quoted in Table 3.

The blockage in the 0.9 velocity ratio case, shown in Figure 6, was 0.0816. To estimate the blockage in the 0.7 velocity ratio case, the blockage in the 0.9 velocity ratio case was multiplied by the ratio of AVRs in the two cases. This results in an estimated blockage for a velocity ratio of 0.7 of 0.079, as quoted in Table 3.

Endwall suction for endwall control

Cases 2 and 3 used endwall suction for endwall control and steady blowing on the suction surface to delay the midspan separation evident in Figure 4(b). These cases have been discussed in detail in Evans *et al* [3].

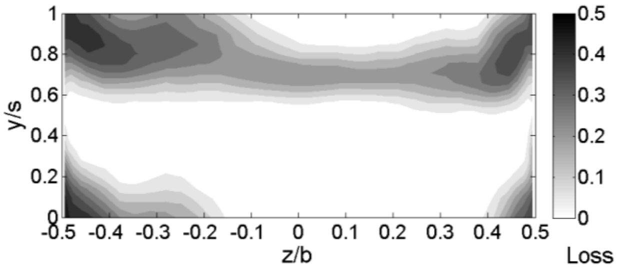

Figure 6. Measured loss contours one chord downstream of cascade for case with tip gaps for endwall control and vortex generator jets on the suction surface. C_μ = 0.45%, V_j/V_1 = 0.9.

As in the case with tip gaps for endwall control, the application of flow control to the suction surface by skewed vortex generator jets induced a cross flow on the surface of the blades in the direction of jet skew. As with the case with tip gaps for endwall control, this flow aggravated the corner separation on the left-hand side of the cascade. The resulting loss core is evident in the loss contours shown in Figure 7(a) for the case with a jet velocity ratio of 0.86, a mass flow ratio of 0.22% and an injected momentum coefficient of 0.42%. The endwall suction in this case was approximately equal to that in the case with just endwall suction, i.e. 0.76% of the cascade inlet mass flow rate.

Figure 7(a) shows a thin wake at midspan, which is consistent with static pressure measurements that, like in the case with tip gaps, indicated a delayed boundary layer separation. The midspan profile loss coefficient, Y_p, for case 2 is 0.026. This is a reduction of 62% relative to the case with endwall suction only. This loss coefficient is also the minimum achieved with steady blowing and fixed endwall suction. The area loss coefficient, Y_a, is 0.096. When corrected for aspect ratio, the area loss, $Y_{a,3.5}$, is 0.064, a 26.5% reduction relative to the baseline case with no endwall or boundary layer control, as quoted in Table 3. The blockage calculated from the wake measurements is 0.053, lower than that estimated in case 1 with tip gaps for endwall control. This is due to the greater effectiveness of endwall suction in removing the corner separations, than tip gaps.

In case 2, endwall suction was fixed at that level required to remove the corner separations in the case with no suction surface flow control. It is therefore referred to as "fixed" endwall suction. The endwall suction mass flow rate was increased on the left-hand side of the cascade to remove the aggravated corner separation that caused the loss core evident in Figure 7(a). By so doing, the AVR was reduced from 1.05 to 1.0. The result was a thin wake across the full span, as shown in Figure 7(b) for the case with a jet velocity ratio of 0.89, a jet mass flow ratio of 0.23% and an injected momentum coefficient of 0.45%. This was the jet velocity ratio that produced the minimum profile loss coefficient, Y_p, of 0.033, a 51.9% reduction relative to the case with endwall suction only. This case, case 3, is described in Table 3 as having "tuned" endwall suction, since the endwall suction mass flow rate was tuned to yield an AVR of 1.0. The suction mass flow rate on the left-hand endwall was increased to 1.03% of the cascade inlet mass flow rate, yielding a total endwall suction mass flow rate of 1.41%. The measured area loss coefficient, $Y_{meas,a}$, is 0.053, significantly lower than that measured with fixed endwall suction. The measured loss coefficient is also quoted in Table 3 for ease of comparison. The total area loss coefficient, Y_a, including the loss associated with endwall suction, however, increased to 0.100. When corrected for aspect ratio, this yields an area loss, $Y_{a,3.5}$, of 0.070. This represents a reduction of 20.3% relative to the case with endwall suction only, as quoted in Table 3.

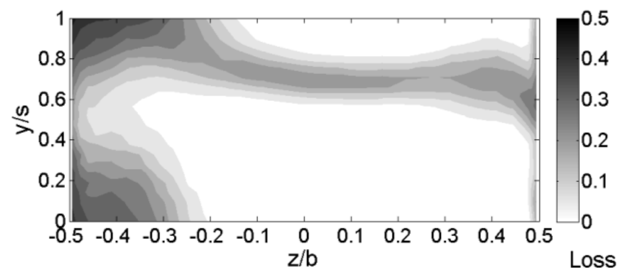

(a)

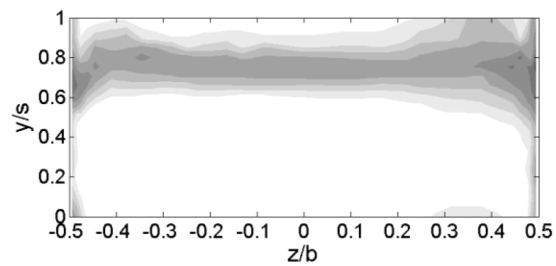

(b)

Figure 7. Measured loss contours one chord downstream of cascade for (a) case 2, with steady VGJs and fixed endwall suction. C_μ = 0.42%, $\dot{m}_{s,end}/\dot{m}_1$ = 0.76% (b) case 3, with steady VGJs and tuned endwall suction. C_μ = 0.45%, $\dot{m}_{s,end}/\dot{m}_1$ = 1.4%.

The blockage calculated for case 3 is 0.036. This is 32% lower than in case 2, due to the absence of the aggravated corner separation.

Unsteady Blowing

Pulsed blowing on the suction surface was studied for the cascade with tip gaps for endwall control. Pulsed blowing was performed over a range of pulse frequencies, for a jet velocity ratio of 0.7. The case quoted in Table 3 as case 4 is for a pulse frequency of 550 Hz. This is equivalent to a reduced frequency,

F^+, defined in equation (15), of 3.7. This is the frequency that corresponds to the minimum profile loss coefficient measured.

$$F^+ = \frac{fL}{V_\infty} \tag{15}$$

where L is the length of the separated region and f is the forcing frequency.

A comparison of case 4 with case 1 enables the direct comparison of pulsed blowing on the suction surface with steady blowing, as both cases use tip gaps for endwall control. The profile loss coefficient, Y_p, measured in case 4 is 0.042. This is a reduction of 57.3% relative to the case with tip gaps only. This is only slightly less than the 61.2% reduction achieved with steady blowing (case 1). In case 4, however, the mass flow ratio is 0.12%, notably lower than the 0.18% required with steady blowing. The injected momentum coefficient is also notably lower – 0.18% in case 4 compared with 0.28% in case 1.

No exit area traverse was conducted with pulsed control, and so no data is available for the area loss coefficient, Y_a.

Boundary Layer Suction

In the final case included in Table 3, the application of suction to both the suction surface/endwall corners and the suction surface boundary layer was studied. This case, case 5, is described in detail in [3]. In this case, the application of suction to the suction surface did not induce any spanwise flow and did not therefore aggravate the left-hand corner separation as in cases 1 and 2, with blowing. Loss contours are shown for case 5 in Figure 8. No loss cores are evident on the endwalls. The suction velocity ratio for this case is 0.61, the suction mass flow ratio is 0.17%[1]. With no aggravated corner separation, the mass flow rate aspirated from the endwalls was the same as that aspirated from the endwalls in the case with endwall suction only, i.e. 0.71% of the passage inlet mass flow rate.

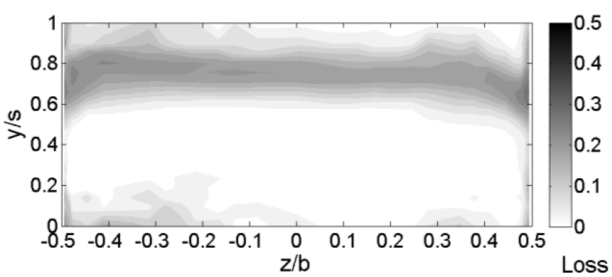

Figure 8. Measured loss contours one chord downstream of cascade for case 5, with boundary layer and endwall suction. *MR* = 0.17%, $\dot{m}_{s,end} / \dot{m}_1$ = 0.71%.

[1] This includes only the mass flow rate sucked from the suction surface, and not that sucked from the suction surface/endwall corners.

The case shown in Figure 8 is for the suction mass flow ratio for which the minimum profile loss coefficient was measured. This profile loss coefficient is 0.037. This is a reduction of 46.2% relative to the case with endwall suction only. This is not as great as the reduction achieved with blowing, shown as Cases 2 and 3. The area loss coefficient, Y_a, is 0.075. When corrected for aspect ratio, the area loss coefficient, $Y_{a,3.5}$, is 0.058, a reduction of 33.9% relative to the baseline case with no endwall or suction surface flow control. This is a significantly greater loss reduction than achieved with blowing in either case 2 or 3. The greater loss reduction is despite the higher profile loss coefficient and thicker wake at midspan, and is due to the absence of an aggravated corner separation and the additional endwall suction required to control it.

The blockage in case 5 is 0.053. This is as high as in case 2 with fixed endwall suction and an aggravated corner separation. This is due to the thicker midspan wake, which generates the same blockage as the aggravated corner separation in case 2, despite generating less loss.

ESTIMATED EFFICIENCY IMPROVEMENT

The reductions in the loss coefficient, $Y_{a,3.5}$, quoted in Table 3 and discussed above were converted into improvements in polytropic efficiency, relative to the baseline case. This calculation assumed a stage with a flow coefficient of 0.5, a stage loading of 0.4 and a baseline polytropic efficiency of 80%. A low efficiency was assumed for the baseline case due to the separations present. The resulting improvement in the polytropic efficiency, calculated from the loss reductions, is quoted in Table 4. The increase in polytropic efficiency is quoted in percentage points of efficiency. Case 1 is quoted in italics due to the estimation of the loss coefficient, as described above. Case 4 is not included in the table since no area loss coefficient was calculated for this case.

Table 4. Potential polytropic efficiency improvements as a result of loss reductions measured.

Case	% $Y_{a,3.5}$ reduction	Polytropic efficiency increase
1	*35.9%*	*16.9%*
2	26.6%	11.8%
3	20.3%	8.8%
5	34.0%	15.8%

The results quoted in Table 4 show that substantial gains in polytropic efficiency are possible with the use of flow control. These potential efficiency increases are, however, relative to a baseline case that has significant separation, and cannot be expected in a compressor with an unseparated baseline. To realize the efficiency increase quoted in Table 4 in a real compressor, a highly loaded blade with similar levels of baseline separation would need to be designed with flow control. The polytropic efficiency improvement would then be relative to this blade row without control, rather than a conventional blade with no separation. The benefit relative to the conventional blade would then be an increase in stage loading.

As expected, the cases yielding the largest increases in polytropic efficiency are the two cases with the largest loss reduction, cases 1 and 5. Of these two cases, case 5 is the more desirable flow, due to the presence of the aggravated corner separation and the blockage associated with it, in case 1.

CYCLE ANALYSIS METHODOLOGY

The full engine cycle was modeled using the cycle analysis tool GSP 11, supplied by the Dutch National Aerospace Laboratory (NLR) [19]. Flow control was applied to a single stage of the high-pressure compressor of a generic two-shaft turbofan model within GSP. The various input parameters for the model are shown in Table 5.

Table 5. Input parameters for two-shaft turbofan GSP model.

Fan:	
Design bypass ratio	5.05
Design pressure ratio	1.65
Design polytropic efficiency	93.5%
Low-pressure compressor:	
Design pressure ratio	1.495
Design polytropic efficiency	91.5%
High-pressure compressor:	
Design pressure ratio	11.98
Design polytropic efficiency	88.3%
Combustion chamber:	
Design combustion efficiency	99.5%
Design point relative pressure loss	4.0%
High-pressure turbine:	
Design isentropic efficiency:	92.0%
Low-pressure turbine:	
Design isentropic efficiency:	90.0%

Since individual blade rows are not defined within the model, the blade row to which flow control was applied was defined somewhat arbitrarily at 10% of enthalpy rise through the high-pressure compressor. Blowing and suction mass flow rates were modeled as bleeds: positive for suction and negative for blowing. Endwall suction, boundary layer suction and boundary layer blowing (negative bleed) were all therefore applied at 10% of the enthalpy rise through the compressor, as fractions of the compressor mass flow rate.

In the cases with blowing, in addition to the jets themselves, the jet supply was modeled as a bleed located at a higher stage. This location was determined as that sufficient to supply air at a stagnation pressure that would drive the jets to the desired Mach number. This Mach number was calculated using the experimentally measured jet velocity ratio, injected momentum coefficient and the assumption of a Mach number of 0.75 at the inlet to the flow-controlled blade row.

The bleed location was determined, as a fraction of enthalpy rise through the compressor, using an iterative process that assumed the jet static temperature and density to be equal to the static temperature and density at the bleed location. The jet stagnation pressure was calculated from the static pressure at the bleed location using a discharge coefficient of 0.85 to model the secondary air system.

In calculating the jet Mach number, a scaled mass flow ratio was calculated for the modeled compressor. This differs from the mass flow ratio used in the cascade experiments since the analysis procedure used assumes only the same velocity ratio and injected momentum coefficient as the experiments. The scaled mass flow ratio, jet Mach number normalized by the inlet Mach number to the blade row, M_j/M_1, and the jet supply location, as a fraction of enthalpy rise through the high-pressure compressor, are quoted in Table 6 for the four blowing cases described in Table 3.

Table 6. Mach ratio, scaled mass flow rate and bleed location for blowing cases studied.

Case #	1	2	3	4
V_j/V_1	0.70	0.86	0.89	0.71
C_μ	0.28%	0.42%	0.45%	0.18%
Cascade $\dot{m}_j/\dot{m}_1$	0.18%	0.22%	0.23%	0.12%
M_j/M_1	0.68	0.81	0.84	0.69
Scaled $\dot{m}_j/\dot{m}_1$	0.21%	0.29%	0.31%	0.14%
Bleed location	0.17	0.21	0.23	0.17

The location at which the suction mass flows were re-injected into the gas path was determined as that for which the static pressure equals the pressure at which the secondary air system delivers the aspirated air, once again assuming a discharge coefficient of 0.85. This analysis assumes a ratio of inlet area to endwall suction slot area that is equal to that in the cascade facility. The results of this analysis are shown in Table 7 for all the suction flows.

All the bleeds modeled in the cycle analysis model are summarized in Table 8 for each case studied. Jets are shown as negative bleeds. Bleed location is shown as a percentage of the enthalpy rise through the high-pressure compressor.

With the bleeds defined to model the cost of flow control, the polytropic efficiency of the high-pressure compressor was adjusted until the engine thrust matched that produced by the baseline engine with no bleeds. The increase in polytropic efficiency over the baseline is then the polytropic efficiency increase required to compensate for the cost of flow control.

Table 7. Re-injection location for suction flows.

Case #	2	3	5	
Suction flow	Endwall	Endwall	Blade	Endwall
$\dot{m}_s/\dot{m}_1$	0.76%	1.41%	0.16%	0.71%
M_s/M_1	0.36	0.67	0.61	0.34
Reinjection location	0.098	0.093	0.094	0.098

The analysis described is limited in that it does not consider the number of stages in the compressor and does not therefore consider either bleed or re-injection to occur at specific blade rows. Instead, it has been assumed that bleed and re-injection may be performed at any location in the compressor, quoted as a percentage of enthalpy rise through the compressor. In a real compressor, there are unlikely to be sufficient blade rows to allow for the resolution required by the bleed and re-injection locations quoted in Table 8. It is however believed that the overall behavior of the system is sufficiently well captured by the analysis that this omission is acceptable.

Table 8. Summary of bleed flows.

Case #		1	2	3	4	5
Bleed #1	$\dot{m}$ ratio	-0.18%	-0.22%	-0.23%	-0.12%	0.16%
	location	0.1	0.1	0.1	0.1	0.1
Bleed #2	$\dot{m}$ ratio	0.18%	0.22%	0.23%	0.12%	-0.16%
	location	0.17	0.21	0.23	0.17	0.094
Bleed #3	$\dot{m}$ ratio	-	0.76%	1.41%	-	0.71%
	location	-	0.1	0.1	-	0.1
Bleed #4	$\dot{m}$ ratio	-	-0.76%	-1.41%	-	-0.71%
	location	-	0.098	0.093	-	0.098

CYCLE ANALYSIS RESULTS

The baseline model of the two-shaft turbofan has an (isentropic) efficiency in the high-pressure compressor of 84% at the design point, and a thrust of 254 kN. With a pressure ratio of 11.98, the polytropic efficiency of the high-pressure compressor is 88.29%. The polytropic efficiency increase required to match the thrust with the flow-controlled blade row and associated bleeds is shown in Figure 9 for the 5 cases described in Table 3.

The required efficiency increases shown in Figure 9 are significantly lower than the potential increases quoted in Table 4. This suggests that the potential benefits of flow control significantly out-weigh the cost.

Figure 9 shows that in cases 1 and 4, with tip gaps for endwall control, the cost of flow control to the cycle is 0.018 percentage points in polytropic efficiency in the case of steady blowing and 0.013 percentage points in the case of pulsed blowing. The efficiency increase required to match thrust with pulsed blowing is lower than that with steady blowing due to the reduced mass flow rate required for control. The experiments in these cases yielded similar levels of midspan profile loss reduction and can therefore be assumed to yield comparable benefits to the cycle. The use of tip gaps for endwall control, however, did result in substantial blockage in the suction surface/endwall corner to which the jets were skewed, as shown in Figure 6.

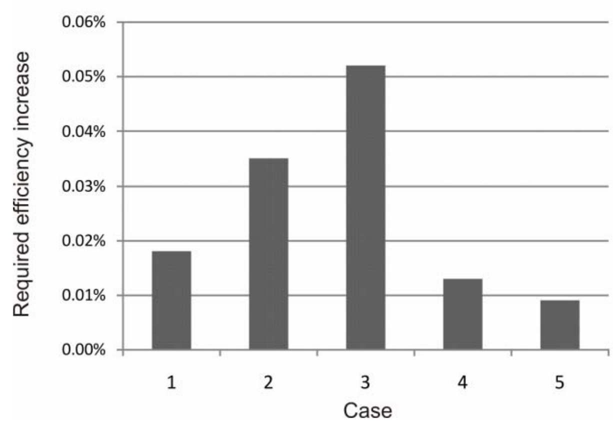

Figure 9. Compressor polytropic efficiency increase required to match thrust, as a result of flow control, for cases described in Table 3.

The cost saving of pulsed blowing over steady blowing is small: just 0.005 percentage points in efficiency. This is unlikely to be sufficient to off-set the challenges associated with implementing pulsed control in a compressor.

In cases 2 and 3, with endwall suction used for endwall control, Figure 9 shows that the efficiency increase required to match thrust goes up with endwall suction. With fixed endwall suction and still high levels of blockage in the corner, the cost is shown in case 2 to be 0.035 percentage points in polytropic efficiency, 0.017 percentage points higher than the comparable case with tip gaps for endwall control (case 1). With additional suction to remove the aggravated corner separation, the efficiency increase required is shown in case 3 to have increased to 0.052 percentage points.

Case 5 shows the case with suction on the suction surface and endwalls. The cost of control in this case is shown in Figure 9 to be a required efficiency increase of 0.009 percentage points. By comparing case 5 with case 2, it is evident that the cost of suction for suction surface boundary layer control is lower than the cost of blowing with vortex generator jets. These two cases have approximately the same mass flow rate sucked from the endwalls and so their difference is entirely due to the differing cost of suction surface control in the two cases. This difference is due to the smaller pressure difference required to achieve suction than blowing. This causes the reinjection location in the suction case, 0.6% of enthalpy rise upstream of the flow controlled blade row, to be closer to the flow controlled blade row than the bleed location in the blowing case, which is 7% enthalpy rise downstream of the flow controlled blade row. The suction case was also shown in Table 4 to yield a greater potential benefit to the cycle – 15.8 percentage points in polytropic efficiency, relative to 11.8 percentage points in case 2.

The required efficiency increase associated with case 5 is notably lower than that associated with case 3 – the only other case with a thin and uniform wake downstream of the blade. The efficiency improvement calculated from the loss measurements and quoted in Table 4 is also higher in case 5 than case 3, due to the lower level of endwall suction resulting from the absence of the aggravated corner separation in case 5.

The results quoted represent the best case due to the application of bleed and re-injection at the optimal location, rather than at the front of the nearest blade row. However, the analysis also assumed corner separations that were measured in a cascade. Due to inlet skew, the corner separations in a real compressor will be smaller than those measured in the cascade. In this sense therefore, the results represent a worst case.

CONCLUSIONS

A series of experiments has been conducted to evaluate flow control within a compressor cascade. Both steady and pulsed vortex generator jets were evaluated with both tip gaps and endwall suction for endwall control. Boundary layer suction was also evaluated. The jet and suction mass flow rates measured in the experiments were used to model a single flow controlled blade row within the high pressure compressor of a turbofan engine using cycle analysis software.

The experimental results show that steady vortex generator jets, pulsed vortex generator jets, and boundary layer suction are all able to delay a separation occurring on a compressor blade at high incidence, reducing the midspan profile loss coefficient by between 46% and 62%. The greatest profile loss reduction was achieved with steady vortex generator jets, while the lowest reduction was achieved with boundary layer suction.

In addition to the profile loss coefficient, however, an area loss coefficient was calculated by averaging the loss over the full blade span. This loss coefficient also included the loss associated with the mixing of the jet with the freestream and that associated with suction, both on the suction surface and in the suction surface/endwall corners. The reduction in this loss coefficient was converted into a polytropic efficiency improvement by making assumptions about the stage in which the flow controlled blade row was located. The polytropic efficiency was increased by 8.8 percentage points using steady blowing on the suction surface and endwall suction for control of the corner separations. By using suction on the suction surface, however, together with endwall suction, an increase in the polytropic efficiency of 15.8% was achieved. The lower efficiency improvement achieved with blowing is partly due to the increased endwall suction required to remove an aggravated corner separation resulting from a spanwise flow induced by the skewed jets.

The suction and blowing mass flow rates measured in these experiments, both on the suction surface and the endwalls, were used to model bleeds in a model of the engine cycle. The objective of this analysis was to identify the cost of flow control to the cycle in each of the flow control cases studied. This analysis showed that pulsed blowing on the suction surface yields a lower increase in polytropic efficiency required to match thrust than steady blowing, but the difference is small: just 0.005 percentage points. The lowest required efficiency increase was calculated for the case with suction on the suction surface and endwalls. This required efficiency increase was 0.009 percentage points in polytropic efficiency, 0.041 percentage points lower than the only blowing case that also produced a thin and uniform wake. The reason for the low efficiency penalty associated with boundary layer suction is the small pressure difference required to drive suction, which allows reinjection of the aspirated air a short distance upstream of the flow controlled blade row.

These results recommend boundary layer suction over blowing for suction surface flow control in a compressor, both from the point of view of the blade performance and the cost of control to the cycle.

The required polytropic efficiency increases calculated using the cycle analysis are significantly lower than the potential increases calculated from the loss reductions measured. This suggests that the potential benefits of flow control significantly out-weigh the cost.

ACKNOWLEDGMENTS

The experimental work reported here was supported by funding under the Sixth Research Framework Program of the European Union, Project ADVACT (Advanced Actuation Concepts), Contract No. 502844. The experimental work was performed at the Whittle Laboratory, University of Cambridge, United Kingdom. Sven-Jürgen Hiller of MTU Aero Engines is acknowledged for his design of the blade used in the cascade.

REFERENCES

[1] Culley, D. E., Bright, M. M., Prahst, P. S., and Strazisar, A. J., (2003) “Active Flow Separation Control of a Stator Vane Using Surface Injection in a Multistage Compressor Experiment,” GT2003-38863, *Proceedings of ASME Turbo Expo*, Atlanta, GA.

[2] Kirtley, K.R., Graziosi, P., Wood, P., Beacher, B., and Shin, H.-W., (2004) “Design and Test of an Ultra-Low Solidity Flow-Controlled Compressor Stator,” GT2004-53012, *Proceedings of ASME Turbo Expo*, Vienna, Austria.

[3] Evans, S., Hodson, H., Hynes, T. and Wakelam, C., (2010) “Flow Control in a Compressor Cascade at High Incidence,” *Journal of Propulsion and Power*, Vol. 26, No. 4, pp 828-837.

[4] Evans, S., Hodson, H., Hynes, T., Wakelam, C., and Hiller S-J, (2010) “Controlling Separation on a Simulated Compressor

Blade using Vortex Generator Jets," *Journal of Propulsion and Power*, Vol. 26, No. 4, pp 819-827.

[5] Reijnen, D.P., (1997) "Experimental Study of Boundary Layer Suction in a Transonic Compressor," *Ph.D. Thesis, MIT*, Cambridge, MA, USA.

[6] Merchant, A., (2002) "Aerodynamic Design and Performance of Aspirated Airfoils," *Proceedings of ASME Turbo Expo*, Amsterdam, The Netherlands.

[7] Gbadebo, S.A., Cumpsty, N.A. and Hynes, T.P., (2004) "Three-Dimensional Separations in Axial Compressors," *Proceedings of ASME Turbo Expo*, Vienna, Austria.

[8] Dean, R.C., Jr., (1954) "The Influence of Tip Clearance on Boundary Layer Flow in a Rectilinear Cascade," *MIT Report* No. 27-3.

[9] Lakshminarayana, B. and Horlock, J.H., (1967) "Leakage and Secondary Flow in Compressor Cascade," *Aeronautical Research Council Reports and Memoranda* 3483, 1967.

[10] Gbadebo, S.A., (2003) "Three-dimensional separations in compressors," *PhD dissertation*, Department of Engineering, University of Cambridge, Cambridge, UK.

[11] Hergt A., Meyer, R. and Müller, M.W., (2008) "Loss reduction in compressor cascades by means of passive flow control," *Proceedings of ASME Turbo Expo*, Berlin, Germany.

[12] Hecklau, M., Wiederhold, O., Zander, V., King, R., Nitsche, W., Huppertz, A. and Swoboda, M., (2010) "Active Separation Control with Pulsed Jets in a Critically Loaded Compressor Cascade," AIAA 2010-4252, *5th Flow Control Conference*, Chicago, IL.

[13] Gmelin, C., Steger, M., Huppertz, A., Swoboda, M. and Thiele, F., (2010) "Unsteady RANS Simulations of a Highly Loaded Low Aspect Ratio Compressor Stator Cascade with Active Flow Control," GT2010-22516, *Proceedings of ASME Turbo Expo*, Glasgow, UK.

[14] Peacock, R.E., (1971) "Boundary-Layer Suction to Eliminate Corner Separation in Cascades of Aerofoils," *Aeronautical Research Council Reports and Memoranda* 3663.

[15] Evans, S., (2009) "Flow Control in Compressors," *Ph.D. Thesis, University of Cambridge*, Cambridge, UK.

[16] Evans, S., Coull, J., Haneef, I., and Hodson, H., (2010) "Minimizing the loss produced by a turbulent separation using vortex generator jets," AIAA-2010-4590, *5th Flow Control Conference*, Chicago, IL.

[17] Selby, G.V., Lin, J.C., and Howard, F.G., (1992) "Control of low-speed turbulent separated flow using jet vortex generators," *Experiments in Fluids*, Vol. 12, pp. 394-400.

[18] Sieverding, C., Maretto, L., Lehthaus, F., and Lawaczeck, O., (1974) "Design and Calibration of Four Probes for Use in the Transonic Turbine Cascade Testing," Technical Note 100, *Von Karmen Institute for Fluid Dynamics*, Rhode Saint Genèse, Belgium.

[19] Visser, W.P.J., and Broomhead, M.J., (2000) "GSP – A Generic Object-Oriented Gas Turbine Simulation Environment," *ASME Turbo Expo*, Munich, Germany.